Two-Photon excited fluorescence microscopy of ocular fundus for the interpretation of fundus autofluorescence analysis *in vivo*

S. Peters [1], L. Deutsch [1], M. Hammer [1], D. Schweitzer [1], J. Dawczynski [2]

[1] University Hospital Jena, Department of Exp. Ophthalmology, Jena, Germany; [2] University Hospital AöR Leipzig, Department of Ophthalmology, Leipzig, Germany

University Hospital Jena

PS36-330

Introduction

Two-photon excited fluorescence (TPEF) imaging of ocular tissue has recently become a promising tool in ophthalmology for diagnostic and research purposes. The feasibility and the advantages of TPEF imaging, namely deeper tissue penetration and improved high-resolution imaging of microstructures, have been demonstrated lately using human ocular samples [1-4]. The autofluorescence properties of endogenous fluorophores in ocular fundus tissue are well known from spectrophotometric analysis [5-7]. But fluorophores, especially when it comes to fluorescence lifetime, typically display a dependence of their fluorescence properties on local environmental parameters. Hence, a more detailed investigation of ocular fundus autofluorescence ideally in vivo is of utmost interest. The aim of this study is to determine the fluorescence emission spectra and lifetimes of endogenous fluorophores in ex vivo porcine ocular fundus samples by means of two-photon excited fluorescence spectrum and lifetime imaging microscopy (FSIM/FLIM). In addition, more detailed insights into fundus autofluorescence (FA) properties might serve as a reference in order to improve FA analysis in vivo using a confocal scanning laser ophthalmoscope (cSLO) in combination with FLIM [6].

Methods

Shortly after enucleation young porcine eyes were kept on ice in DMEM cell culture medium (Invitrogen). The paramacular fundus samples were prepared by transscleral trephine biopsy (ø 5 mm, GlaxoSmithKline).

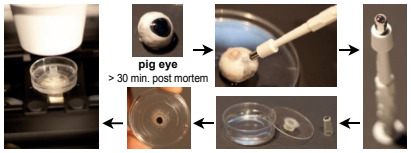

An inverted multiphoton laser scanning microscope (Axio Observer Z.1 and LSM 710 NLO, Carl Zeiss) in combination with a femtosecond Ti:Sapphire laser (80 MHz; 140 fs; λ_{ex}=760 nm) (Chameleon Ultra, Coherent Inc.) and a single photon counting setup consisting of two hybrid photomultiplier tubes (HPM-100-40) in non-descanned operation together with a SPC 150 TCSPC board (Becker & Hickl) has been employed. The lifetime imaging measurements are based on the principle of time correlated single photon counting (TCSPC) [8].

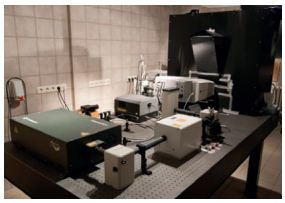

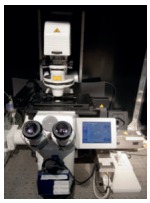

A detailed description of the FLIM-cSLO setup can be found elsewhere [6]. The lifetime decay curves of all FLIM images have been analyzed using the SPCImage software (Becker & Hickl). Chi-square was used as a goodness-of-fit criterion.

Results

TPEF has been employed to investigate the autofluorescence properties of porcine ocular fundus *ex vivo* samples by means of FSIM and FLIM.

Fluorescence Spectrum Imaging Microscopy

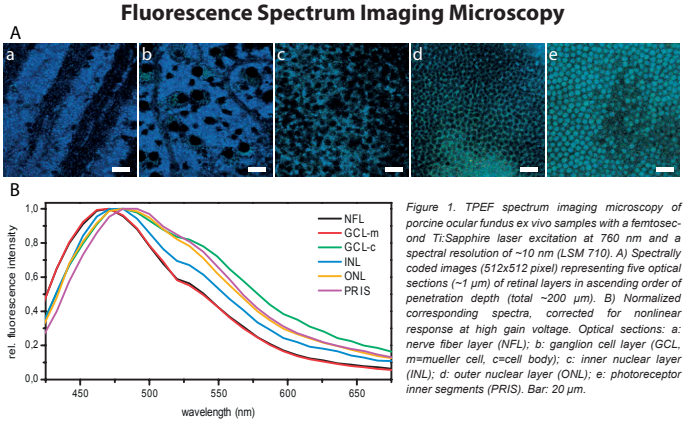

Figure 1. TPEF spectrum imaging microscopy of porcine ocular fundus ex vivo samples with a femtosecond Ti:Sapphire laser excitation at 760 nm and a spectral resolution of ~10 nm (LSM 710). A) Spectrally coded images (512x512 pixel) representing five optical sections (~1 µm) of retinal layers in ascending order of penetration depth (total ~200 µm). B) Normalized corresponding spectra, corrected for nonlinear response at high gain voltage. Optical sections: a: nerve fiber layer (NFL); b: ganglion cell layer (GCL, m=mueller cell, c=cell body); c: inner nuclear layer (INL); d: outer nuclear layer (ONL); e: photoreceptor inner segments (PRIS). Bar: 20 µm.

The two-photon excited autofluorescence spectra from all imaged porcine retinal layers can mainly be explained by a superposition of NADH and FAD fluorescence. The peak around 450 to 500 nm, dominating in all layers, can be assigned to NADH and the peak around 530 nm to FAD fluorescence. The absorption of NADH up to 500 nm explains the spectral redshift as well as the ratioshift [6].

Fluorescence Lifetime Imaging Microscopy

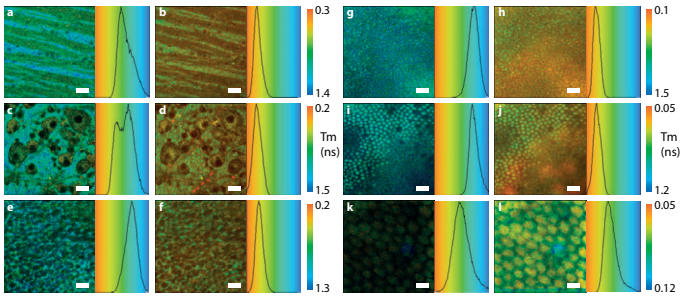

Figure 2. TPEF lifetime imaging microscopy of porcine ocular fundus ex vivo samples with a femtosecond Ti:Sapphire laser excitation at 760 nm and two detection channels: 500-550 nm (left column), 550-700 nm (right column). The images (256x256 pixel) represent six optical sections (~1 µm) of retinal layers in ascending order of penetration depth (total ~220 µm). False colors indicate the amplitude-weighted mean fluorescence lifetime (Tm) of a bi-exponential approximation. Next to each image its Tm distribution is depicted. Optical sections: a,b: nerve fiber layer; c,d: ganglion cell layer; e,f: inner nuclear layer; g,h: outer nuclear layer; i,j: photoreceptor inner segments; k,l: retinal pigment epithelium. Bar: 20 µm.

Except for the RPE cells, all optical sections showed similar values of mean Tm (amplitude-weighted mean fluorescence lifetime) in the range of 900-1100 ps (500-550 nm) and 400-600 ps (550-700 nm), respectively. The Tm of RPE cells is considerably shorter and identical in both spectral windows (~80 ps). The Tm distribution of the GCL showed two maxima with an absolute difference in the mean Tm of around 400 ps (500-550 nm) and 150 ps (550-700 nm), respectively.

Representative fluorescence lifetimes of ex vivo porcine retinal layers

500-550 nm		550-700 nm		500-700	
A1: ~73 % T1: ~0,4 ns	*free* **NADH** *bound*	A1: ~85 % T1: ~0,2 ns	*bound* **FAD** *free*	A1: ~98 % T1: ~0,07 ns	**Melanin**
A2: ~27 % T2: ~2,4 ns		A2: ~15 % T2: ~2,0 ns		A2: ~2 % T2: ~0,6 ns	

All retinal layers display similar fluorescence decays except the RPE cells

Table 1. Fluorescence lifetime parameters of individual optical sections of porcine ocular fundus ex vivo samples.

		NFL	GCL	GCL-c	GCL-m	INL	ONL	PRIS	RPE
500-550 nm	a1 (%)	72,5 ± 5,7	74,1 ± 6,9	80,0 ± 3,4	66,6 ± 3,7	73,1 ± 4,1	68,6 ± 3,4	76,2 ± 3,3	98,4 ± 0,9
	τ1 (ns)	0,39 ± 0,05	0,39 ± 0,06	0,36 ± 0,04	0,43 ± 0,05	0,40 ± 0,06	0,39 ± 0,07	0,43 ± 0,06	0,07 ± 0,01
	a2 (%)	27,5 ± 5,7	25,9 ± 6,9	20,0 ± 3,4	33,4 ± 3,7	26,9 ± 4,1	31,4 ± 3,4	23,8 ± 3,3	1,6 ± 0,9
	τ2 (ns)	2,35 ± 0,20	2,36 ± 0,25	2,22 ± 0,24	2,48 ± 0,20	2,36 ± 0,24	2,64 ± 0,26	2,33 ± 0,27	0,61 ± 0,23
550-700 nm	a1 (%)	83,4 ± 2,4	85,3 ± 3,0	86,7 ± 2,2	81,9 ± 2,2	85,7 ± 2,1	88,6 ± 2,1	91,6 ± 2,5	98,3 ± 1,2
	τ1 (ns)	0,23 ± 0,03	0,21 ± 0,04	0,20 ± 0,04	0,23 ± 0,04	0,20 ± 0,04	0,17 ± 0,03	0,17 ± 0,03	0,07 ± 0,01
	a2 (%)	16,6 ± 2,4	14,7 ± 3,0	13,3 ± 2,2	18,1 ± 2,2	14,3 ± 2,1	11,4 ± 2,1	8,4 ± 2,5	1,7 ± 1,2
	τ2 (ns)	1,98 ± 0,20	1,93 ± 0,25	1,78 ± 0,19	2,13 ± 0,18	1,98 ± 0,22	2,07 ± 0,24	1,81 ± 0,19	0,54 ± 0,22

NFL: nerve fiber layer; GCL: ganglion cell layer (c: cell body, m: mueller cell); INL: inner nuclear layer; ONL: outer nuclear layer; PRIS: photoreceptor inner segments; RPE: retinal pigment epithelium. Values are given as mean ± SD for n=3.

Fluorescence Lifetime Imaging *in vivo*

Representative fluorescence lifetimes of young healthy subjects *in vivo*, integrated over the retina and a parapapillary area are: T1 ~60 ps; T2 ~400 ps; T3 ~3,0 ns; A1 ~88 %; A2 ~10 % (490-560 nm) and T1 ~70 ps; T2 ~400 ps; T3 ~2,2 ns; A1 ~ 80 %; A2 ~18 % (560-700 nm). These lifetimes can be assigned to RPE cells, the retina and the lens.

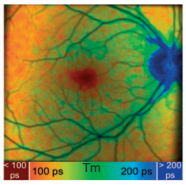

Figure 3. FLIM-cSLO image (6x6 mm) of a human ocular fundus in vivo. (exc: 448 nm; em: 490-560 nm; Tm: amplitude-weighted mean fluorescence lifetime - tri-exponential approximation in false colors)

Conclusion

TPEF in combination with LSM is very well suited to investigate the autofluorescence of ocular fundus tissue with threedimensional spatial resolution. By our first results, we characterized the stationary and time-resolved autofluorescence properties of individual anatomical structures of ex vivo porcine retina samples. Since all retinal layers exhibit biexponential autofluorescence decays, we were able to achieve a more precise characterization compared to a present in vivo approach by FLIM-cSLO. With a TPE at 760 nm all retinal layers only slightly differ from each other regarding their fluorescence properties except for the RPE cells, which is due to the presence of identical endogenous fluorophores namely NADH and FAD. This implicates a great potential for detecting and localizing physiological and pathological metabolic alterations. Individual fluorescence lifetimes are in very good agreement with *in vivo* FLIM-cSLO measurements, which are thereby confirmed. Further investigations using TPEF microscopy might provide a more specific diagnostics of metabolic / pathological alterations in ocular fundus tissue.

References

[1] B. G. Wang, K. Koenig, I. Riemann et al., "Intraocular multiphoton microscopy with subcellular spatial resolution by infrared femtosecond lasers," Histochemistry and cell biology, 126(4), 507-15 (2006).

[2] M. Han, G. Giese, S. Schmitz-Valckenberg et al., "Age-related structural abnormalities in the human retina- choroid complex revealed by two-photon excited autofluorescence imaging," Journal of biomedical optics, 12(2), 024012 (2007).

[3] B. G. Wang, A. Eitner, J. Lindenau et al., "High-resolution two-photon excitation microscopy of ocular tissues in porcine eye," Lasers in surgery and medicine, 40(4), 247-56 (2008).

[4] O. La Schiazza, and J. F. Bille, "High-speed two-photon excited autofluorescence imaging of ex vivo human retinal pigment epithelial cells toward age-related macular degeneration diagnostic," Journal of biomedical optics, 13(6), 064008 (2008).

[5] F. C. Delori, C. K. Dorey, G. Staurenghi et al., "In vivo fluorescence of the ocular fundus exhibits retinal pigment epithelium lipofuscin characteristics," Investigative ophthalmology & visual science, 36(3), 718-29 (1995).

[6] D. Schweitzer, S. Schenke, M. Hammer et al., "Towards metabolic mapping of the human retina," Microscopy research and technique, 70(5), 410-9 (2007).

[7] D. Schweitzer, S. Jentsch, S. Schenke et al., "Spectral and time-resolved studies on ocular structures," Proceedings of SPIE-OSA Biomedical Optics. 6628, 6628_6. (2007)

[8] W. Becker, [The bh TCSPC Handbook] Becker & Hickl GmbH, Berlin(2010).

Acknowledgement

We are very grateful to Jens Haueisen for his support in providing the microscopic equipment.

Conflict of Interests

1. no, 2. no, 3. no, 4. no, 5. no